

# Understanding thermochemical aspects of the magnesium metal fuel subjected to hygrothermal aging with varied oxygen flow rates

Juyoung Oh<sup>1</sup> and Jack J. Yoh<sup>1</sup>

<sup>1</sup>Department of Aerospace Engineering, Seoul National University  
Seoul, Korea 08826

## 1 Introduction

With fossil fuel reserves running out in addition to the increasing environmental concerns, solutions for sustainable energy sources are sought. Amongst the known alternative energy sources, metal fuels have been regarded as a promising candidate for resolving the environmental issues as they release considerable amount of heat energy without the carbon dioxide formation. Bergthorson et al. [1] have selected those metal fuels based on their 1) sufficient reactivity with atmospheric oxygen for energy purposes, 2) costs, 3) toxicity, and 4) abundant reserves on earth. Such metals included lithium (Li), boron (B), magnesium (Mg), aluminum (Al), silicon (Si), iron (Fe), and zinc (Zn). The current study focuses on Mg particles, which are then subjected to two distinct aging conditions, namely a drying condition containing silica gels within a storage pack and an atmospheric condition having moisture. Such aging conditions affect the thermochemical properties and change the reaction kinetic paths. The combustion efficiency is also investigated while varying the O<sub>2</sub> flow rate to obtain O<sub>2</sub> rich and lean condition dependencies.

The work presented marks a kinetic analysis by combining the statistical information on the activation energy values for Mg as a metal fuel. It is found that atmospheric moisture enables Mg oxidation even at O<sub>2</sub>-lean condition while decreasing the reactivity by creating Mg hydroxides as the product of such hygrothermal aging. However, thermally aged Mg recovered heat of reaction in accordance with the aging duration due to the decreased activation energy at increasing oxide film thickness. Also, at O<sub>2</sub>-rich condition, thermally aged Mg showed an increase in the heat of reaction, presumably due to more Mg particles involved in the oxidation process. Therefore, the reaction paths of the pristine Mg need to be subsequently modified as both hydroxides and oxides form during the hygrothermal aging at different O<sub>2</sub> flow rates.

## 2 Experimental details and kinetics calculations

### 2.1 Materials

Mg powder (purity: 99.9%, particle size: 40 $\mu$ m) was utilized for thermochemical analysis. Also, Mg powder was aged to identify the temperature as well as humidity effects on the thermal properties of Mg.

The samples were packed with silica gels for drying conditions, and another batch was kept without the moisture absorber for atmospheric conditions. The two types of Mg were stored in the oven at the temperature of 71 °C for various thermal (accelerated) aging periods. Table 1 shows the aging conditions.

Table 1: Utilized samples and specific aging conditions.

Sample label	Aging conditions		
	Temperature	Drying treatment	Period
Mg #0 (Pristine)	-	-	-
Mg #1, Mg #1-D	71 °C	Mg #1-D	1 week
Mg #2, Mg #2-D		Mg #2-D	2 weeks
Mg #3, Mg #3-D		Mg #3-D	3 weeks
Mg #4, Mg #4-D		Mg #4-D	4 weeks

## 2.2 Thermal analysis

The various thermodynamic characteristics for aged Mg metal fuels were obtained by applying the DSC experiments. The utilized instrument was DSC 3+ model from Mettler Toledo. In general, metals can release substantial heats during the oxidation reaction while moderate heat energy must be supplied simultaneously. Thus, the temperature range was 30~600°C at various heating rates of 1, 2, 3, 4, and 5 °C/min. During the experiments, oxygen gas was provided into the furnace at different flow rates of 50 mL/min ( $\dot{V}_{50}$ ) and 100 mL/min ( $\dot{V}_{100}$ ) each to identify the combustion efficiency depending on oxygen flow conditions. Mg powder samples were put into the 40  $\mu$ L standard aluminum crucibles as evenly as possible to avoid any concentrated heat localization during the measurement. The utilized sample weight was empirically obtained around 0.3~0.4mg, suitable for preventing any self-heating problem. The conducted experiments strictly followed the International Confederation for Thermal Analysis and Calorimetry Kinetics Committee's recommendations [2] to obtain further the reliable results.

## 2.3 Chemical reaction kinetics extraction via the Friedman-isoconversional method

Based on the obtained DSC results, kinetic parameters were extracted by applying the Friedman-isoconversional method [3]. Under non-isothermal conditions which utilize various heating rates ( $\beta = dT/dt$ ), the differential isoconversional method can be represented by the heating rate and the reaction rate, given by Eq. (1). Taking the logarithm at both sides of Eq. (1), the activation energy ( $E_a$ ) and pre-exponential factor ( $\ln[f(\alpha)A_\alpha]$ ) can be calculated by the slope and y-intercept, respectively, as shown by Eq. (2). Here, the x-axis is  $1/T_{\alpha,i}$  and the y-axis denotes  $\ln[(\beta_i^* d\alpha/dt)_{\alpha,i}]$  each.

$$\beta \frac{d\alpha}{dT} = A_\alpha \exp\left(\frac{-E_\alpha}{RT}\right) f(\alpha) \quad (1)$$

$$\ln\left[\left(\beta_i \frac{d\alpha}{dT}\right)_{\alpha,i}\right] = \ln[f(\alpha)A_\alpha] - \frac{E_\alpha}{RT_{\alpha,i}} \quad (2)$$

where  $\alpha$ ,  $T$ , and  $R$  indicate the reaction progress, the absolute temperature (K), and the gas constant (J/K·mol) each. The subscript  $\alpha$  and  $i$  represent isoconversional values and heating rate conditions.

## 2.4 Statistical analysis

The extracted activation energy on the reaction conversion were utilized for statistical analysis. Based on the activation energy on the whole range of the reaction progress, a normal distribution was obtained

for each sample. Here, the calculated average value ( $\mu$ ) and the standard deviation ( $\sigma$ ) were employed to identify the aging effects as well as O<sub>2</sub> supply conditions on Mg with respect to the statistical aspect.

### 3 Results

#### 3.1 Thermochemical behaviors of a pristine sample

Figure 1 shows the DSC thermograms for unaged Mg powder, namely Mg #0, under 50 mL/min of O<sub>2</sub> flow rate around the furnace, at five different heating rate conditions. Similar to other solid energetic materials, Mg #0 showed the heating rate effect, indicating the initiation as well as the peak intensity of the exothermic reactions is proportional to the heating rate. The calculated heat of reaction and the peak temperature for the current samples are depicted in Table 2. The provided exothermic reactions denote the oxidation process of Mg particles as given in Eq. (3).

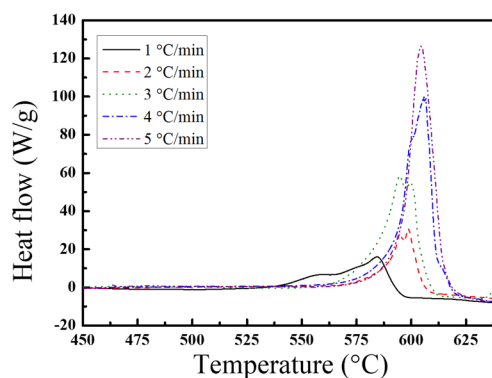
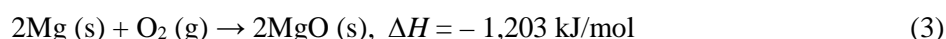


Figure 1: DSC thermograms of Mg #0 (pristine) at five different heating rates (1, 2, 3, 4, and 5 °C/min).

#### 3.2 Aging effects on thermal properties

Now, the nonisothermal DSC measurements were conducted for aged Mg metal particles. The extracted thermal properties viz. heat of reaction and the peak temperature of unaged and 4 weeks aged samples are provided in Table 2. The heat of reaction tended to decrease in accordance with the aging duration. Mg #4-D only contained about 80% of the value of Mg #0. For peak temperatures, the aged one had slightly increased values except for the low heating rate of 1 °C/min. Hygrothermal aging effects on peak temperatures could also be found; Mg #4-D tended to have lowered peak temperatures up to 7°C when compared to the values for Mg #4. Mg particles with drying treatments showed better reactivity in general although the heat performance was similar regardless of the storage conditions, which can be resulted from the effect of the oxide film thickness on the metal particles.

Table 2: Aging effects on thermal parameters of Mg metal fuels.

Sample Name	Heat of reaction, $\Delta H$ (kJ/g)	Peak temperature (°C)
Mg #0	22.34±0.76	585.11 (1 °C/min), 596.33 (2 °C/min), 599.77 (3 °C/min), 607.72 (4 °C/min), 606.58 (5 °C/min)
Mg #4	18.52±1.03	582.84 (1 °C/min), 600.76 (2 °C/min), 610.91 (3 °C/min), 608.39 (4 °C/min), 611.48 (5 °C/min)

Mg #4-D	18.03±1.03	580.03 (1 °C/min), 598.02 (2 °C/min), 603.57 (3 °C/min), 609.35 (4 °C/min), 606.37 (5 °C/min)
---------	------------	--

### 3.3 Aging effects on statistical parameters

Figure 2 illustrates normal distributions to the observed Mg metal fuels on the extracted activation energy values. Figures 2(a) and 2(b) are correlated to the obtained results conducted at  $\dot{V}_{50}$  and  $\dot{V}_{100}$ , respectively. Aged Mg metals tended to have decreased average values of the activation energy whereas standard deviations were increased. Under the O<sub>2</sub>-rich condition, as given by Fig. 2(b), the corresponding effects were much noticeable. For metals, the aging process can be explained by the process of oxidization on the surface of the particle. For Mg, a stabilization process right after a sudden increase can follow when oxide film thickness ranges over 0.1  $\mu\text{m}$  [4] as shown in Fig. 2(c), which signifies that the aged samples in the current study have formed the oxide film which is thicker than at least 0.1  $\mu\text{m}$ .

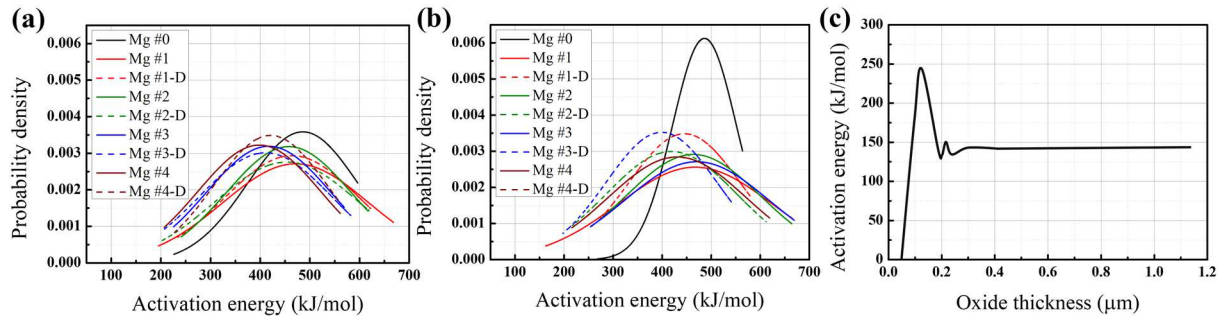


Figure 2: Aging effects on the activation energy for Mg, represented by a normal distribution and the activation energy as a function of oxide thickness of Mg. (a) The O<sub>2</sub>-lean (50 mL/min), (b) the O<sub>2</sub>-rich (100 mL/min), and (c) the relationship between activation energy and oxide thickness of Mg.

### 3.4 O<sub>2</sub> flow rate effects – O<sub>2</sub>-rich conditions as tested

Table 3 shows obtained thermal parameters for the aged Mg treated with drying condition. Regarding the heat of reaction, Mg #1-D showed a decrease up to 30% of its pristine value. The degree of decrease was much rapid in  $\dot{V}_{100}$  condition. After another week of aging elapsed (Mg #2-D), however, the released heat tended to recover. This can be explained by the effect of the oxide thickness of Mg; the activation energy starts to decrease and stabilize over 0.1  $\mu\text{m}$  of oxide film (Fig. 2(c)). [4] As the lowering of energy barrier which leads to a lowered activation energy during aging, it becomes easier for the remained Mg to participate in the recovery of the heat of reaction. Also, the O<sub>2</sub>-rich condition showed a continuously increasing trend, whereas in the O<sub>2</sub>-lean condition, the released heat tended to decrease. Likely the higher amount of O<sub>2</sub> supply increases the probability of oxidation of thermally aged Mg. Meanwhile, except for the Mg #1-D case, peak temperatures increased at all O<sub>2</sub>-rich conditions.

Table 3: O<sub>2</sub> flow rate effects on thermochemical parameters of Mg #n-D.

Sample Name	Heat of reaction, $\Delta H$ (kJ/g)		Peak temperature (°C)	
	$\dot{V}_{50}$	$\dot{V}_{100}$	$\dot{V}_{50}$	$\dot{V}_{100}$
Mg #1-D	17.81±1.52	15.48±1.41	608.85 (3 °C/min)	596.05 (3 °C/min)
Mg #2-D	19.49±1.83	17.29±1.39	608.46 (3 °C/min)	610.52 (3 °C/min)
Mg #3-D	19.14±1.54	19.00±1.62	605.58 (3 °C/min)	605.72 (3 °C/min)
Mg #4-D	18.03±1.03	19.32±1.37	603.57 (3 °C/min)	604.40 (3 °C/min)

In Fig. 3, Mg #0 showed a clear difference in the statistical results depending on the O<sub>2</sub> flow rate. The value of  $\sigma$  showed an inverse trend to the O<sub>2</sub> flow rate whereas the  $\mu$  was almost constant. Figure 4 elucidates the observed changes in normal distributions depending on the O<sub>2</sub> flow rate. Here, Fig. 4(a) and 4(b) show the results for Mg metals aged under atmospheric conditions while Fig. 4(c) and 4(d) indicate drying conditions. O<sub>2</sub>-lean and O<sub>2</sub>-rich conditions provided a noticeable difference in  $\mu$  of Mg metals. For Mg #n cases, the  $\mu_{50}$  tended to move fast to lower values with a decreased  $\sigma$ . For Mg #n-D cases, however, an opposite tendency is found. In other words, the  $\mu_{100}$  had a tendency to shift quickly towards lower values. Depending on the presence of the moisture content during its storing conditions, the kinetics distribution can change as metal substances can be reactive to the presence of either oxygen or moisture. The results for Mg #n in Fig. 4(a) and 4(b) showed the opposite tendency to the results of Mg #0 and Mg #n-D, which signifies that the existence of the moisture can significantly alter the combustion reaction paths for Mg metal fuels by forming hydroxides as opposed to oxides. During the heating process, Mg hydroxide further decomposes into MgO and H<sub>2</sub>O at 332 °C without oxygen supply as shown in Eq. (4). Subsequently, the O<sub>2</sub>-lean condition can give rise to a stoichiometric reaction of magnesium. However, thermally aged Mg treated at drying condition needs to be supplied with more oxygen for an efficient combustion to proceed as an additional source of oxygen supply such as Mg(OH)<sub>2</sub> is in absence.



## 4 Conclusion

This work has demonstrated the aging effects and combustion efficiency of Mg metal fuels based on the thermochemical analysis. The degradation of the reactivity due to accelerated aging at different O<sub>2</sub> flow conditions is observed as a decrease in heat of reaction and the increased peak temperature during the exothermic chemical reaction. Also, the activation energy value of Mg decreased with aging indicating the formation of the oxide film with its thickness well over 0.1  $\mu\text{m}$ . Depending on the presence of atmospheric moisture during aging, the reaction kinetics are considerably affected by the abundance of oxygen supplied. Hygrothermally aged Mg showed the decreasing trend of activation energy in O<sub>2</sub>-lean conditions, which is due to more hydroxides generation. However, the aged Mg at dry condition showed lowered activation energy in O<sub>2</sub>-rich conditions due to the formation of more oxides. Therefore, the performance of Mg in its thermochemical characteristics can degrade upon the exposure to moisture during the oxidation process, and the full exothermic reaction paths can change due to the appearance of hydroxides. For effective utilization of Mg-based metal fuels, a close attention must be paid to both the moisture condition as well as the oxidation condition.

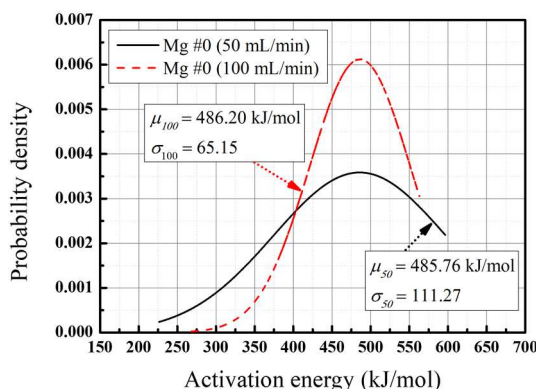


Figure 3: O<sub>2</sub> flow rate effects on the activation energy for Mg #0, represented by a normal distribution.

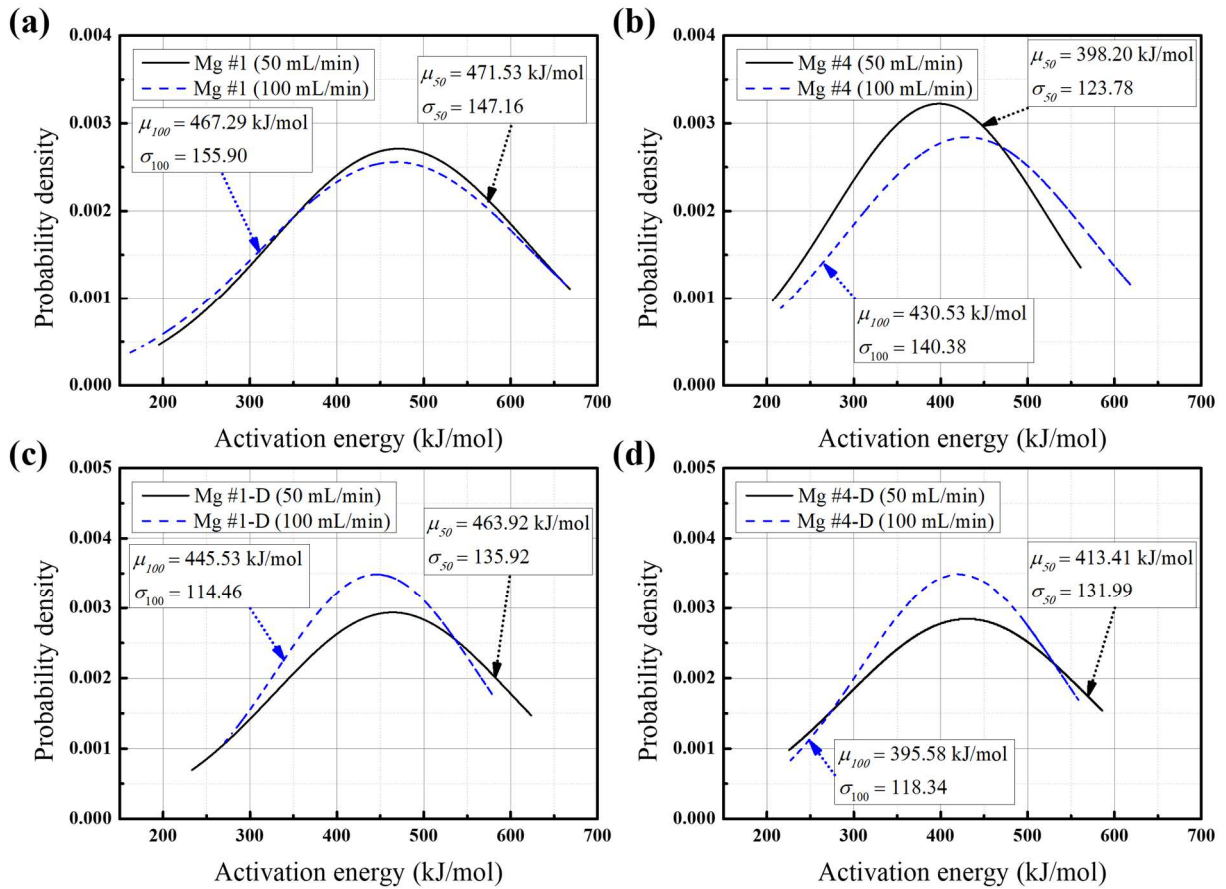


Figure 4: O<sub>2</sub> flow rate effects on the activation energy for aged Mg metal fuels represented by a normal distribution. (a) Mg #1, (b) Mg #4, (c) Mg #1-D, and (d) Mg #4-D.

## ACKNOWLEDGMENTS

This work was supported by the National Research Foundation of Korea (NRF2020R1F1A1072007) contracted through IAAT and IOER at Seoul National University.

## References

- [1] Bergthorson JM. (2018). Recyclable metal fuels for clean and compact zero-carbon power. *Prog. Energ. Combust.* 68:169.
- [2] Vyazovkin S, Burnham AK, Criado JM, Pérez-Maqueda LA, Popescu C, Sbirrazzuoli, N. (2011). ICTAC Kinetics Committee recommendations for performing kinetic computations on thermal analysis data. *Thermochim. acta*, 520:1.
- [3] Oh J, Jang SG, Yoh JJ. (2019) Towards understanding the effects of heat and humidity on ageing of a NASA standard pyrotechnic igniter. *Sci. Rep.*, 9:1.
- [4] Nie H, Schoenitz M, Dreizin EL. (2016). Oxidation of magnesium: implication for aging and ignition. *J. Phys. Chem. C*, 120:974.